Doklady Earth Sciences, Vol. 388, No. 1, 2003, pp. 72–76. Translated from Doklady Akademii Nauk, Vol. 388, No. 2, 2003, pp. 237–241.

GEOPHYSICS

Development of the Method of Cataclastic Analysis of Shear Fractures for Tectonic Stress Estimation

Yu. L. Rebetskii

Presented by Academician Yu.G. Leonov May 28, 2002

Received May 31, 2002

Within the framework of solving the principal inverse problem of tectonophysics, stress tensor parameters are calculated (restored) with the help of data on a set of shear fractures (with grooves), which are measured in outcrops, or seismological data on earthquake focal mechanisms [1]. The method of cataclastic analysis [3–5] has the following essential advantage: it includes physically substantiated criteria for the selection of shear fractures (focal mechanisms of earthquakes) for the grouping of homogeneous samples used for the subsequent calculation of stress tensor parameters. The practice of cataclastic analysis demonstrates that it is quite sufficient to use a homogeneous sample of 10–15 shear fractures (focal mechanisms) for the spatiotemporal identification of quasi-homogeneously deformed macroblocks and the calculation of four parameters of stress tensor, namely, three Euler angles, which determine orientations of three main axes of the tensor, and the Lode–Nadai coefficient μ_σ, which characterizes relationship between the main tensor values. However, the currently existing algorithm of cataclastic analysis does not allow calculation of all stress tensor components. For example, its invariants, such as the confining pressure $p = -\frac{1}{3}(\sigma_1 + \sigma_2 + \sigma_3)$ and the maximal tangential stress modulus $\tau = 0.5(\sigma_1 - \sigma_3)$, remain unknown. Therefore, this calculation algorithm should be treated as an algorithm for the first stage of calculation of stress tensor parameters.

The present communication demonstrates that the calculation of unknown stress tensor parameters should mainly be based on homogeneous samples of shears formed at the first calculation stage. Therefore, let us consider laboratory experimental results on the brittle destruction of specimens of two types. Type 1 samples were initially undeformed, whereas type 2 samples contained some surfaces with decreased strength or incisions [7, 8]. These experiments demonstrated a rather wide scatter of data points over the σ_{nn}, τ_n (normal and tangential stresses acting on shear surfaces) parametric area for a wide range of rock specimens (Fig. 1). The application of Byerlee relationships (bold line in Fig. 1) for the study of fracture morphology (brittle destruction) allows one to reveal only a predominant position of rupture surfaces and average values of parameters that determine their strength properties. The range of the possible scatter of shear-plane orientations cannot be determined based on Byerlee's theory. At the same time, results of the first stage of stress calculation demonstrate that a scatter, sometimes significant, is always present in the homogeneous sample of shear fractures (or focal mechanisms). Hence, the formation of shear planes (activation of previously existing, or creation of new, shear planes), which are oriented at different angles, is a fundamental property of deformation in fractured rocks. As demonstrated in [6, 9], the upper boundary of the data point cluster (Fig. 1) determines the relationship of the brittle strength limit of rocks with the internal friction coefficient, which depends on the normal stress value, whereas the lower boundary characterizes the minimal surface friction value in existing ruptures, provided that the surface friction coefficient is constant and the adhesion stress is

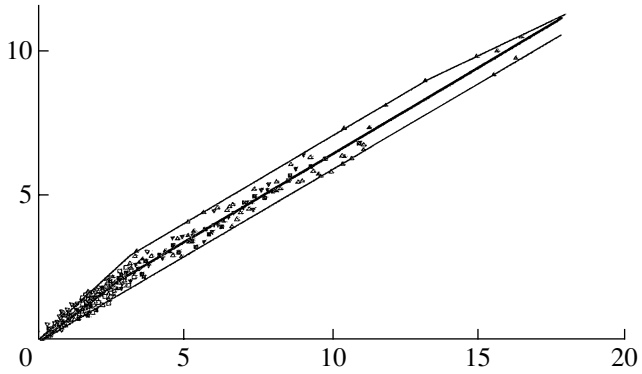

Fig. 1. Results of experimental investigations of the role of friction in rocks at high pressure. Normal stress modulus (kbar) is given along the abscissa. Bold line is based on the approximation of Byerlee's observations. Thin lines are based on the approximation proposed in the present communication.

Schmidt Joint Institute of Physics of the Earth, Russian Academy of Sciences, ul. Bol'shaya Gruzinskaya 10, Moscow, 123995 Russia

close to zero (thin lines in Fig. 1). Within the normal stress range (3–15 kbar) on the shear surface (central sector of Fig. 1), both lines bounding the data point cluster from the top and bottom are parallel to the known approximation of laboratory observation results ($\tau_n + 0.6\sigma_{nn} = 0.5$ kbar) proposed by Byerlee as a criterion of the brittle destruction of rocks. It may be assumed for this sector that friction sliding along fracture walls in the specimens is realized according to the Coulomb–Mohr's law at similar values of the static surface friction coefficient ($k_s = 0.6$ at rest) and different values of adhesion (≤1 kbar).

With respect to fractured rock massifs, we shall use the principal characteristic features of destruction revealed in the laboratory experiments and assume that values of parameters, which govern the process in the rock massifs, may differ from laboratory modeling values. Let us assume for the consolidated crust at depths of more than 5 km (pressure >2–3 kbar) that the value of adhesion along an existing fracture or fault surface (τ_c^k, where k is the number of the shear) and along a weakened surface can vary within the range $0 \le \tau_c^k \le \tau_c$. In this case, the maximal value of adhesion at the shear surface (τ_c) governs the effective strength limit of rock massifs. Note that the τ_c value must be less than the experimental value (1 kbar). Conditions on the fracture walls at $\tau_c = 0$ characterize the lower limit of relationship between the normal and tangential stresses. On reaching this limit, the respective weakened surfaces (fault and fractures) can be involved in brittle destruction. Let us denote this relationship as the minimal strength limit of dry friction or as a relationship that determines the beginning of brittle destruction. Thus, the following equation is valid for fractures activated in rock massifs (the formation of a weakened surface and relative displacement of walls can be separated in time):

$$\tau_n + k_s\sigma_{nn} = \tau_c^k \text{ at } 0 \le \tau_c^k \le \tau_c,\ \sigma_{nn} < 0, \qquad (1)$$

where k_s and τ_c are parameters governing effective strength properties of rock massifs during the brittle destruction. They depend on the deformation history and recent structural-dynamic state of tectonospheric areas.

An analysis of a Mohr's circle diagram (Fig. 2) within the framework of hypotheses proposed above demonstrated an importance of the opening angle AOC ($2\Delta\alpha$) formed by points of intersection of the large Mohr's circle, which is constructed on the basis of algebraically maximal and minimal values of the main stresses, with the line that determines the minimal strength of the existing fractures ($\tau_n + k_s\sigma_{nn} = 0$). The $2\Delta\alpha$ value depends on the scatter of shear-plane orientations in homogeneous samples, relative to axes of the main stresses that were calculated after the first stage of stress reconstruction. This inversely correlates with intensity of the stressed state (Mohr's circles are

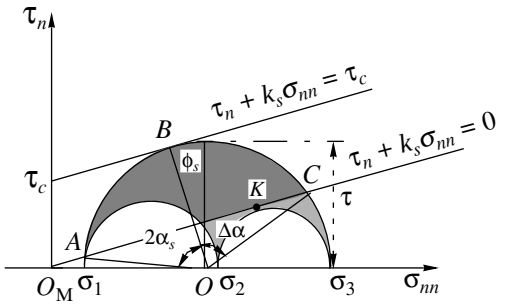

Fig. 2. Mohr's circle diagram with lines of the minimal (dry friction) and maximal strength limits. Dark gray area corresponds to the region of admissible positions of shear planes for the adhesion range of $0 \le \tau_c^k \le \tau_c$. The light gray area corresponds to the region of possible states at arbitrary planes. ($\phi_s = \arctan k_s$) is the angle of surface friction; ($\Delta\alpha$) is the opening angle for two points that characterize shears with the maximal and minimal normal stresses in Mohr's diagram. Negative values of the normal stress on an inclined plane are plotted on the right side of the horizontal axis.

located to the right of the σ_{nn} axis). The latter conclusion is crucial for solving the problem formulated at the beginning of the present communication. Based on the geometry of the Mohr's circle diagram presented in Fig. 2, the following expressions can be obtained for the confining effective pressure and maximal tangential stress modulus:

$$p = \frac{\tau_c(\tilde{\tau}_n^K + k_s\tilde{\sigma}_{nn}^K)}{k_s\left[\operatorname{cosec} 2\alpha_B - \frac{k_s\mu_\sigma}{3} - (\tilde{\tau}_n^K + k_s\tilde{\sigma}_{nn}^K)\right]},$$
$$\tau = \frac{\tau_c}{\operatorname{cosec} 2\alpha_B - \frac{k_s\mu_\sigma}{3} - (\tilde{\tau}_n^K + k_s\tilde{\sigma}_{nn}^K)}, \qquad (2)$$

where α_B is the angle between the normal to the shear plane, which is characterized by the maximal strength ($\left(\alpha_B = \frac{1}{2}\arctan\frac{1}{k_s}\right)$), and the axis of the algebraically maximal main stress σ_1. Values $\tilde{\sigma}_{nn}^K$ and $\tilde{\tau}_n^K = \tilde{\sigma}_{nt}^K$ are normalized stresses for shear with minimal strength (Fig. 2, point K) obtained through division of the respective stress-deviator components ($\tau\tilde{\sigma}_{nn}^K = \sigma_{ij}^K - \delta_{ij}p$, where δ_{ij} is the Kronecker symbol) by the maximal tangential stress modulus τ. The normalized stresses $\tilde{\sigma}_{nn}^K$ and $\tilde{\sigma}_{nt}^K$ are completely determined by results of the first stage of stress tensor calculation:

$$\tilde{\sigma}_{nn}^K = (1-\mu_\sigma)(l_{n1}^K)^2 - (1+\mu_\sigma)(l_{n3}^K)^2,$$
$$\tilde{\tau}_n^K = \tilde{\sigma}_{nt}^K = (1-\mu_\sigma)l_{n1}^K l_{t1}^K - (1+\mu_\sigma)(l_{n3}^K l_{t3}^K), \qquad (3)$$

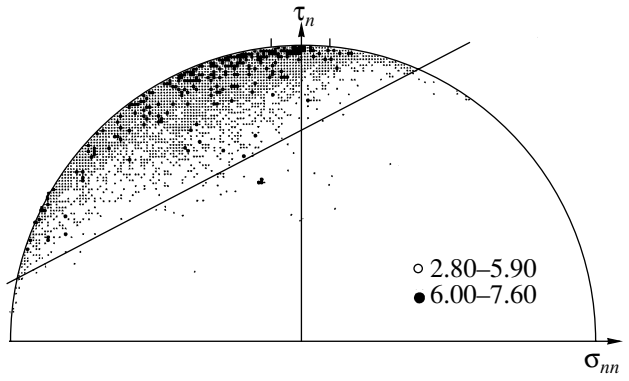

Fig. 3. Summary Mohr's diagram for the plane in an earthquake focus based on criterion (4).

where l_{ni}^K and l_{ti}^K are direction cosines of vectors **n** (normal to the shear plane) and **t** (direction of the tangential stress on this plane) in the coordinate system related to the main stress axes (i = 1, 2, 3); μ_σ is the Lode–Nadai coefficient of the stress tensor. Let us note that the confining pressure p should be considered an effective pressure representing the difference between the total tectonic pressure (including lithostatic) and the fluid pore pressure.

Expressions (2), which determine values of the confining pressure and maximal tangential stress, contain two unknown scalar parameters (the coefficient of surface friction k_s and the maximal effective strength of fractured rock massifs τ_c). It should also be remembered that when p and τ are calculated on the basis of seismological data on earthquake focal mechanisms, the rupture plane realized in the focus is also unknown. In this case, the determination of surface friction coefficient at rest and the identification of one of the nodal planes (with normals **n** and **s**) as a fault plane are interrelated problems. In order to solve these problems, we shall assume that values of the maximal tangential stresses acting on the rupture plane are crucial for its activation. It is these stresses that are responsible for overcoming the friction acting in the fault (1). We assume that the deflection of sliding direction along the rupture plane from the direction of maximal tangential stresses ($\tau_n^i \geq \sigma_{ns}^i > 0$ and $\tau_s^i \geq \sigma_{ns}^i > 0$) is related to an anisotropy within the brittle destruction band (corrugation of the rupture plane) and, possibly, to kinematic constraints caused by disjunctive structure of the environment (intersections with other faults).

The possibility of solving the above-specified problems may be demonstrated by the example of data on 1670 spatiotemporal quasi-homogeneous macroblocks of the Earth's crust in the northeastern seismoactive area of the Pacific (127°–130° E and 26°–30° N). The macroblocks were distinguished on the basis of results of stage 1 calculation by the cataclastic analysis method. Seismological data were taken from the catalogue of earthquake focal mechanisms compiled by the Seismological Survey of Japan for the period from January 1, 1996, to January 5, 2002 (4100 crustal earthquakes with magnitudes of $3 \leq M_w \leq 6.8$). Each of the quasi-homogeneous macroblocks contained 8 to 18 earthquake focal mechanisms. Based on the assumption that the surface friction coefficient k_s is independent of the stressed state, one can construct a Mohr's diagram that summarizes data on stresses on the realized rupture plane for all earthquakes within the studied seismoactive crustal area. For this purpose, Mohr's circles corresponding to each macroblock with a homogeneous stressed state should be shifted by the value $p + \frac{\mu_\sigma}{3}\tau$ along the axis of normal stresses in such a way that their centers coincide with each other. All parameters of the stresses should subsequently be normalized by the tangential stress modulus τ. As a criterion for selection of a rupture plane within an earthquake focus during the summary diagram construction, we shall use the following condition based on expression (1):

$$\tilde{\tau}_n^k + k_s\tilde{\sigma}_{nn}^k \geq \tilde{\tau}_s^k + k_s\tilde{\sigma}_{ss}^k, \quad (4)$$

where $\tilde{\tau}_n^k$ and $\tilde{\tau}_s^k$ are normalized tangential stresses for nodal planes of the kth earthquake center, whereas $\tilde{\sigma}_{nn}^k$ and $\tilde{\sigma}_{ss}^k$ are normal stress counterparts. According to (4) and (1), the nodal plane selected as a rupture in the focus must be characterized by a higher adhesion strength required for its activation. In order to check criterion (4), $k_s = 0.6$ was accepted as an initial approximation value (this value was obtained by Byerlee [6] in experiments with specimens at high pressures). The results are presented in Fig. 3. One can see that the cluster of data points makes up an elongated zone with its lower boundary inclined at about 60°. Data points for strong earthquakes with $M_w \geq 6$ tend to approach the circle boundary on the Mohr's diagram. Based on the lower boundary of the cluster of data points (Fig. 3), $k_s \approx 0.5$ can be accepted as the value of the surface friction coefficient for the study area.

After the identification of rupture planes within earthquake foci based on criterion (4) and the calculation of surface friction coefficient, we again processed results of stage 1 calculation of stress tensor parameters for 1670 quasi-homogeneous crustal macroblocks in the seismoactive area of Japan based on expressions (2). Thus, we obtained relative values of the effective confining pressure and maximal tangential stress with a precision of the unknown maximal effective adhesion τ_c. The calculations demonstrated a certain dependence of p and τ on the stressed state type. Thus, crustal average values of $\frac{p}{\tau}$ were 1.79, 1.67, and 1.56 for μ_σ = –1, 0, and +1, respectively. On the other hand, as seen from Fig. 2, the p versus τ relationship for seismoactive areas

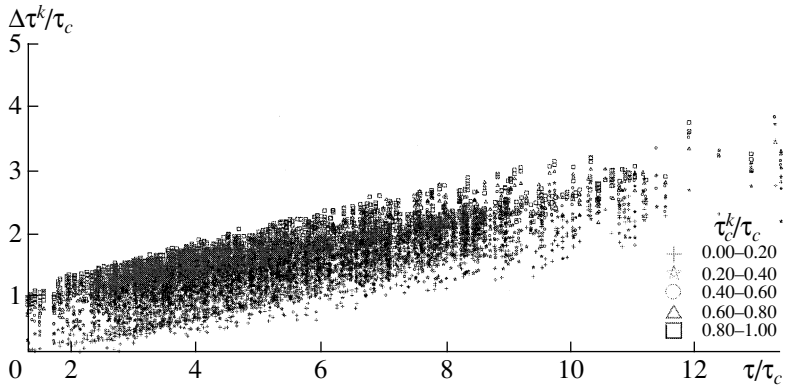

Fig. 4. Stresses discharged on a rupture vs. maximum tangential stresses. Adhesion values in the fault (τ_c^k) are shown by different symbols.

of the Earth's crust during brittle destruction is determined by the following expression:

$$\frac{p}{\tau} = \cos\Delta\alpha\sqrt{\frac{1}{k_s^2}+1} - \frac{\mu_\sigma}{3}, \quad (5)$$

where $\Delta\alpha$ is one-half the opening angle in the Mohr's diagram (Fig. 2). Maximal and minimal values of $\Delta\alpha$ are determined by the respective marginal positions of Mohr's circles for possible stressed states in the Mohr's diagram. For example, $\frac{p}{\tau} = 1 - \frac{\mu_\sigma}{3}$ ($\Delta\alpha \approx 63.4°$) at $\sigma_1 = 0$ and $\frac{p}{\tau} = 2.24 - \frac{\mu_\sigma}{3}$ ($k_s = 0.5$) at $\Delta\alpha \to 0$.

The approach elaborated in the present work makes it possible to determine not only the surface friction coefficient k_s of rock massifs, but also other characteristics of mechanical strength, namely, the value of relative adhesion in the activated rupture plane. Using condition (1) together with (2), we obtain

$$\tau_c^k = \tau_c\frac{(\tilde\sigma_{ns}^k + k_s\tilde\sigma_{nn}^k) - (\tilde\sigma_{ns}^K + k_s\tilde\sigma_{nn}^K)}{\operatorname{cosec}2\alpha_B - \frac{k_s\mu_\sigma}{3} - (\tilde\sigma_{ns}^K + k_s\tilde\sigma_{nn}^K)}. \quad (6)$$

This expression offers the key to calculating some essential earthquake focus parameters. Yamashita [10] assumed that dry friction in a fault is subdivided into the static component k_s, which acts before the activation of the fault, and the dynamic component k_d ($k_d < k_s$), which determines the displacement amplitude along the fault at the rupture stage. Based on this assumption, one can elaborate the following algorithm for the calculation of stresses discharged on the rupture:

$$\Delta\tau^k = \sigma_{ns}^k - \bar\sigma_{ns}^k \text{ at } \sigma_{ns}^k + k_s\sigma_{nn}^k = \tau_c^k,$$
$$\bar\sigma_{ns}^k + k_d\bar\sigma_{nn}^k = 0. \quad (7)$$

Lines above the stress components here indicate assignment to the dynamic stage. Let us note that normal stresses in a fault remain unchanged before and after its activation [2], i.e., $\bar\sigma_{nn}^k = \sigma_{nn}^k$. Together with expressions (2) and (3), this condition allows us to obtain the following expression for the discharged stress $\Delta\tau^k$:

$$\Delta\tau^k = \tau_c\frac{k_s(\tilde\sigma_{ns}^k + k_d\tilde\sigma_{nn}^k) - k_d(\tilde\sigma_{ns}^K + k_d\tilde\sigma_{nn}^K)}{k_s\left[\operatorname{cosec}2\alpha_B - \frac{k_s\mu_\sigma}{3} - (\tilde\sigma_{ns}^K + k_s\tilde\sigma_{nn}^K)\right]}. \quad (8)$$

Figure 4 shows the dependence of discharged stress on the maximal tangential stress modulus. The positive correlation of the discharged stress with τ is a characteristic feature. However, the possible scatter is only three times lower than the maximal value.

Conclusions. Based on experiments with specimens, we suggest that adhesion in faults within rock massifs shows the following range: $0 \le \tau_c^k \le \tau_c$, provided that the surface friction coefficient is constant. This hypothesis made it possible to find the relation of the previously known concept of rock state along the shear fracture surface (Coulomb–Mohr's law for brittle destruction) and its presentation in the form of a Mohr's circle diagram with estimates of stressed state parameters of crustal areas based on stage 1 stress reconstruction. It is this hypothesis that allowed us to elaborate algorithms for the calculation of stress tensor parameters, strength characteristics of fractured rock massifs, and some earthquake focus parameters.

ACKNOWLEDGMENTS

This work was supported by the International Scientific and Technical Center, project no. 1536.

REFERENCES

1. Gzovskii, M.V., *Osnovy tektonofiziki* (Essentials of Tectonophysics), Moscow: Nauka, 1975

2. Osokina, D.N. and Fridman, V.N., in *Polya napryazhenii i deformatsii v zemnoi kore* (Stress and Strain Fields in the Earth's Crust), Moscow: Nauka, 1987, pp. 74–119.
3. Rebetskii, Yu.L., *Materialy soveshchaniya "Strukturnye paragenezy i ikh ansambli"* (Materials of Conf. on Structural Parageneses and Their Assemblages), Moscow, 1997, pp. 144–146.
4. Rebetskii, Yu.L., *Dokl. Akad. Nauk*, 1999, vol. 365, no. 3, pp. 392–395.
5. Rebetskii, Yu.L., in *M.V. Gzovskii i razvitie tektonofiziki* (M.V. Gzovskii and Development of Tectonophysics), Moscow: Nauka, pp. 311–325.
6. Byerlee, J.D., *J. Geophys. Res.*, 1968, vol. 73, pp. 4741–4750.
7. Byerlee, J.D., *Pure Appl. Geophys.*, 1978, vol. 116, pp. 615–626.
8. Stesky, R.M., *Pure Appl. Geophys.*, 1978, vol. 116, pp. 691–704.
9. Rummel, F., Alheid, H.J., and Frong, C., *Pure Appl. Geophys.*, 1978, vol. 116, pp. 743–764.
10. Yamashita, T., *J. Phys. Earth*, 1976, no. 24, pp. 417–444.